APPLICATION OF THE UNDIFFERENCED GNSS PRECISE POSITIONING IN DETERMINING COORDINATES IN NATIONAL REFERENCE FRAMES

Grzegorz Krzan, Katarzyna Stępniak
University of Warmia and Mazury in Olsztyn,
Institute of Geodesy, Oczapowskiego 1, 10-719 Olsztyn, Poland
grzegorz.krzan@uwm.edu.pl

ABSTRACT: In high-accuracy positioning using GNSS, the most common solution is still relative positioning using double-difference observations of dual-frequency measurements. An increasingly popular alternative to relative positioning are undifferenced approaches, which are designed to make full use of modern satellite systems and signals. Positions referenced to global International Terrestrial Reference Frame (ITRF2008) obtained from Precise Point Positioning (PPP) or Undifferenced (UD) network solutions have to be transformed to national (regional) reference frame, which introduces additional bases related to the transformation process.

In this paper, satellite observations from two test networks using different observation time series were processed. The first test concerns the positioning accuracy from processing one year of dual-frequency GPS observations from 14 EUREF Permanent Network (EPN) stations using NAPEOS 3.3.1 software. The results were transformed into a national reference frame (PL-ETRF2000) and compared to positions from an EPN cumulative solution, which was adopted as the true coordinates. Daily observations were processed using PPP and UD multi-station solutions to determine the final accuracy resulting from satellite positioning, the transformation to national coordinate systems and Eurasian intraplate plate velocities. The second numerical test involved similar processing strategies of post-processing carried out using different observation time series (30 min., 1 hour, 2 hours, daily) and different classes of GNSS receivers. The centimeter accuracy of results presented in the national coordinate system satisfies the requirements of many surveying and engineering applications.

Key words: PPP, ITRF, ETRF, ESA, IGS

1. INTRODUCTION

To achieve precise positioning using Global Navigation Satellite System (GNSS), two approaches are possible. In regions abundant in Continuously Operating Reference Stations (CORS), the most common is relative positioning (El-Rabbany, 2006). This approach allows to determine precise coordinates of a rover receiver using observations from CORS, which position is known. Since signals reaching both nearby receivers are affected by common disturbing effects, it is possible to use the double-differencing (DD) of observations to eliminate or mitigate most of the systematic errors (Kleusberg 1986, Hofmann-Wellenhof

2003). Although, such solution is relatively straightforward, it also has some significant disadvantages. Due to the limited distance between reference and rover receivers, a dense network of CORS is required, what is costly to establish and operate.

Precise Point Positioning (PPP) based on undifferenced dual-frequency carrier phase observations is an alternative to relative positioning and can provide centimeter accuracy using observations from a single GNSS receiver (Cai and Gao, 2007). This is possible by using precise satellite clock and orbit estimates within the processing and modelling of the systematic effects interfering with range determination between satellites and receivers (Kouba et al., 2001; El-Mowafy, 2009). The PPP using clock and orbit products automatically ties the resulting coordinates to the highly-accurate homogenous global International Terrestrial Reference Frame (ITRF2008). The strategy initially used by scientists studying the condition of ionosphere, the motion of continental plates, time transfer and tropospheric parameters estimation, has recently become popular for surveying, precise positioning and even in precision farming (Zumberge, 1997; Bisnath, and Gao, 2009; Araszkiewicz et al., 2010, Kalita et al., 2014; Roberts et al., 2015; Golaszewski et al., 2017, Paziewski et al., 2017). The reason for this is mainly the simplification of processing using PPP software packages or online automatic services calculating positions based on a submitted Receiver Independent Exchange System (RINEX) observation file. In a single point positioning solution, the phase ambiguities are not possible to fix, so a significant drawback of PPP is a long accuracy-convergence period which is referred to as the time from cold start to a decimeter-level solution (Chen et al., 2009*)*. Studies on PPP indicate that typical convergence time lasts about 30 minutes in standard conditions and will be significantly longer for weak satellite geometry (Dawidowicz and Krzan 2014; Alkan et al. 2015). To overcome this inconvenience, it is possible to resolve DD integer ambiguities in an UD multi-station solution by estimating the fractional cycle biases (FCB) (Ge et al., 2008) or integer-recovery clocks (IRC) (Laurichesse and Mercier, 2007). Furthermore, ambiguity fixing provides accuracy improvement, especially in an east-west direction, in the processing of shorter observation sessions. Geng et al. (2009; 2010) achieved positioning enhancement from 3.8 cm (East), 1.5 cm (North) and 2.8 (Elevation) in a float solution to 0.5 cm, 0.5 cm and 1.4 cm, respectively, after one hour of satellite observations. Along with the development of GNSS systems, several authors studied using GLONASS and Galileo signals in PPP processing (Cai and Gao, 2007; Choy et al., 2013; Rabbou and El-Rabbany, 2015; Afifi and El-Rabbany, 2015). The obtained results indicate that the improvement in accuracy from utilizing combined GNSS observations is evident in cases of weak satellite geometry and short observing sessions. The benefits of combining signals from different GNSS in the processing of daily observations are debatable because it did not visibly improve the positioning accuracy.

The International GNSS Service (IGS) is providing free and open access to their data collection since 1994 (Neilan, 1997; Kouba, 2009). The IGS global tracking network continuously records satellite observations from over 300 permanent GNSS stations provides rich data, processed by Analysis Centers (AC), to compute satellite orbits and clocks products as well as station coordinates and velocities, earth rotation parameters, etc. (IGS, 2015). The IGS final clock and orbit products are currently combined from up to nine ACs using different software packages such as BERNESE, GAMIT, GIPSY, NAPEOS etc. (Lichten, 1995; Gendt et al., 1999; Schenewerk et al., 1999; Marty 2009; Springer et al., 2011). In addition to the application of different programs, the some systematic bias models also differ between AC. The logs containing analysis strategy summaries from different AC indicate that the processing strategies may vary in: double-differencing observations and using un-differenced observations, modeling of 2nd order of ionospheric delays or using the tropospheric model

(Kouba, 2009). The IGS combination of AC products computed involving different approaches and models result in a more robust and precise solution with lower random-like noise averaged out within the combination process.

The International Terrestrial Reference System (ITRS), in which IGS products are expressed, is a kinematic system because the station coordinates, which are the physical representation of the system, change several centimeters per year. Thus, it is necessary to define the coordinates for a specific epoch, taking into account local velocities and vertical movements (Petit and Luzum, 2010). The actual realization of ITRS is ITRF2008, has been recently replaced by ITRF2014 (Altamimi et al., 2016). To maintain the stability of coordinates in time, the International Association of Geodesy (IAG) sub-commission EUREF adopted the European Terrestrial Reference System (ETRS89) which is consistent with ITRS at the epoch $t_0 = 1989.0$ and fixed to a stable part of the Eurasian Plate (Bosy, 2013). EPN stations are the physical realization of ETRS89. By analyzing position time series from many years of GNSS observations, EPN can provide very accurate station coordinates and velocities in the European Terrestrial Reference Frame (ETRF2000) as well as the transformation parameters between the global ITRF and regional ETRF realizations (Boucher and Altamimi, 2011). Further densification of EPN are generally national CORS networks, which transfer the ETRF2000 to European countries according to a resolution from XXth EUREF symposium in Gävle, Sweden in 2010. In Poland, the ASG-EUPOS network realizes the national geodesic reference frame called PL-ETRF2000 which is consistent with ETRF2000 at epoch 2011.0 and constitutes the reference for satellite measurements for relative positioning.

The relationships between GNSS networks as well as between reference frames are described in detail by Bosy (2013). Szafranek (2012) studied the problem of temporal validity of reference coordinates in Poland, in the context of the reliability of the ETRS89 using the Bernese software DD approach to determine the coordinates and velocities from a four-year observation period collected at ASG-EUPOS sites. The obtained results indicated that, despite small intraplate velocities in Poland, periodical changes to the catalogue coordinates of the ASG-EUPOS are necessary. Bogusz et al. (2012) analyzed the velocity field determined from ASG-EUPOS observations and found many unmodeled effects which diminish the reliability of linear trend velocity determinations.

This study examines UD positioning methods in determining positions in national reference frames. Daily observation periods are used to determine the final accuracy resulting from satellite positioning, the transformation between coordinate systems and the Eurasian intraplate distortion. The one-year period of observations utilized in the study aims to show the seasonal fluctuations of coordinates. Along with additional investigations on sub-daily time series for different classes of GNSS receivers, the results presented in the national coordinate system can be analyzed in terms of geodynamic applications as well as surveying and engineering tasks.

2. PROCESSING STRATEGY APPLIED

The implemented PPP strategy, processed using NAPEOS 3.3.1 software, starts with the pre-processing of observations, followed by actual processing and least squares parameter estimation. In pre-processing, after selecting adequate data, each observation is screened for outliers and cycle slips using linear combinations (LC) and statistical tests. The description of Melbourne-Wübbena (MW) LC and screening for the time difference of the ionosphere observables used by NAPEOS are described in detail in Springer et al. (2011).

The ionospheric-free combination applied in processing uses dual-frequency GNSS pseudorange (*P*) and carrier-phase (*L*) observations (Kouba, 2009):

$$P3 = \frac{f_1^2 P_1 - f_2^2 P_2}{f_1^2 - f_2^2} \tag{1}$$

$$L3 = \frac{f_1^2 \lambda_1 \phi_1 - f_2^2 \lambda_2 \phi_2}{f_1^2 - f_2^2} \tag{2}$$

$$P3 = \rho + c(dT - dt) + T_r + \varepsilon_p \tag{3}$$

$$L3 = \rho + c(dT - dt) + T_r + \lambda N + \varepsilon_L \tag{4}$$

Where:

$P3$	- the ionosphere-free combination of P_1 and P_2 pseudoranges,
$L3$	- the ionosphere-free combination of L_1 and L_2 carrier-phases,
ρ	- geometrical range from satellite to station position,
f_1, f_2	- the L_1 and L_2 frequencies,
dT	- the station receiver clock offset,
dt	- the satellite clock offset,
c	- the speed of light in vacuum,
T_r	- signal neutral-atmosphere delay,
N	- non-integer ambiguity of ionosphere-free carrier-phase
$\lambda_1, \lambda_2, \lambda$	- the wavelengths of L_1, L_2 and $L3$, respectively,
$\varepsilon_P, \varepsilon_L$	- measurement noise, including multipath.

When the IGS orbit and clock products are applied, satellite clocks dt can be considered as known. The tropospheric path delay T_r can be divided into an easily-predictable, thus easy-to-eliminate *a priori*, hydrostatic part, and an estimated in processing wet troposphere delay.

$$T_r^k(t) = m_w(z)T_w(t) + m_d(z)\,T_d\,(t) \tag{5}$$

In NAPEOS, the zenith path delay (ZPD) is computed using the Saastamoinen model with pressure and temperature from the Global Pressure Temperature (GPT) model. The resulting ZPD is subsequently mapped using the dry Global Mapping Function (GMF). These models are described in detail in Boehm et al. (2006, 2007). Other corrections used in this study are (ESOC, 2009):

- Tidal displacement related to solid Earth, pole, ocean and atmospheric tides compliant with the International Earth Rotation and Reference Systems Service (IERS2010) standards (Petit and Luzum 2010),
- Phase wind-up and relativistic effects.

The solution of linearized observation equations using least square estimation is the last step in determining parameters by PPP. At this stage, ambiguities are non-integer as the observations from stations were processed individually. To recover integer ambiguity as in the UD multi-station solution, the network method by Blewitt (1989) is utilized in NAPEOS. In this approach, the first step is forming the DD ambiguities per baseline, neglecting the network geometry. The computations start with determination of DD Melbourne-Wübbena wide-lane ambiguities. Subsequently, sorted MW ambiguities are fixed, based on their probability function value (ESOC, 2009; Collins, 2008):

$$P_0 = 1 - \sum_{n-1}^{\infty} erfc\left(\frac{n-(b-I)}{\sqrt{2}\sigma}\right) - erfc\left(\frac{n+(b-I)}{\sqrt{2}\sigma}\right) \tag{6}$$

where:

$$erfc(x) = \frac{2}{\sqrt{\pi}} \int_x^{\infty} e^{-t^2} dt \tag{7}$$

    b   - MW DD ambiguity estimate in wide-lane cycles,
    I   - nearest integer of MW DD ambiguity estimate,
    σ   - MW DD ambiguity sigma in wide-lane cycles.

Successfully-fixed MW DD ambiguities allow for forming and fixing narrow-lane (NL) ambiguities. The condition of independence between ambiguities is checked using the modified Gram-Schmidt method after sorting them from high to low fixing probability. Finally, an independent set of ambiguities are introduced to a normal equation system (ESOC, 2009). A more accurate solution is obtained using an iterative process of least square adjustment which improves ambiguity fixing in subsequent runs, thus resulting in very high accuracy parameters after the iteration process.

To express the resulting coordinates in ETRF2000, it is necessary to perform a Helmert transformation using formulae from Boucher and Altamimi (2011):

$$\begin{Bmatrix} X_{ETRF} \\ Y_{ETRF} \\ Z_{ETRF} \end{Bmatrix} = \begin{Bmatrix} X_{ITRF} \\ Y_{ITRF} \\ Z_{ITRF} \end{Bmatrix} + \begin{Bmatrix} T_X \\ T_Y \\ T_Z \end{Bmatrix} + \begin{Bmatrix} D & -\omega_z & \omega_y \\ -\omega_z & D & -\omega_x \\ -\omega_y & \omega_x & D \end{Bmatrix} \begin{Bmatrix} X_{ITRF} \\ Y_{ITRF} \\ Z_{ITRF} \end{Bmatrix} \tag{8}$$

Where $\{T_X, T_Y, T_Z\}$ is the translation vector, D is the scale factor and ω_x, ω_y, ω_z represents rotations around *X*, *Y*, *Z* axes, respectively. In Table 1, the transformation parameters are shown. As they are expressed at epoch 2000.0, they should be propagated to the epoch of measurement using:

$$P(t_c) = P(2000.0) + P(t_c - 2000.0) \tag{9}$$

Table 1. Transformation parameters from ITRF2008 to ETRF2000 at epoch 2000.0 and their rates/year (Boucher and Altamimi, 2011)

ITRF Solution	T_X [mm]	T_Y [mm]	T_Z [mm]	D [10^{-9}]	ω_x [mas]	ω_y[mas]	ω_z[mas]
ITRF2008	52.1	49.3	-58.5	1.34	0.891	5.390	-8.712
Rates	0.1	0.1	-1.8	0.08	0.081	0.490	-0.792

3. DATA SET PROCESSED

The first test network is a subset of 14 EPN stations also belonging to the ASG-EUPOS network (Table 2, Fig. 1). All stations are class A EPN stations distributed around Poland.

Table 2. EPN / ASG-EUPOS stations post-processed in the study. Receiver and antenna models, and ETRF2000 intraplate velocities (EPN).

STATION	Receiver	Antenna and dome type		ETRF RATES [MM/YEAR]		
				dN	dE	dH
BOGI	JAVAD TRE_G3T DELTA	ASH701945C_M	SNOW	0.1	-0.5	-0.8
BOR1	TRIMBLE NETRS	AOAD/M_T	NONE	-0.2	-0.3	-1.2
BYDG	TRIMBLE NETR9	TRM59900.00	SCIS	-0.2	-0.6	-0.8
GWWL	TRIMBLE NETR9	TRM59900.00	SCIS	-0.4	-0.6	-1.5
JOZ2	LEICA GRX1200GGPRO	LEIAT504GG	NONE	0.1	0.0	-0.6
KATO	TRIMBLE NETR5	TRM57971.00	TZGD	-3.7	0.0	-1.7
KRA1	TRIMBLE NETR5	TRM57971.00	NONE	0.0	-0.4	-0.5
LAMA	LEICA GRX1200+GNSS	LEIAT504GG	LEIS	0.1	-0.5	-1.0
LODZ	TRIMBLE NETR9	TRM59900.00	SCIS	0.1	0.0	-0.9
REDZ	TRIMBLE NETR9	TRM59900.00	SCIS	-0.3	-0.2	-0.8
SWKI	TRIMBLE NETR9	TRM59900.00	SCIS	0.1	-0.6	-2.3
USDL	TRIMBLE NETR9	TRM59900.00	SCIS	0.0	-0.2	-1.2
WROC	LEICA GR25	LEIAR25.R4	LEIT	0.1	-0.6	-0.5
ZYWI	TRIMBLE NETR9	TRM59900.00	SCIS	0.4	-0.4	-1.0
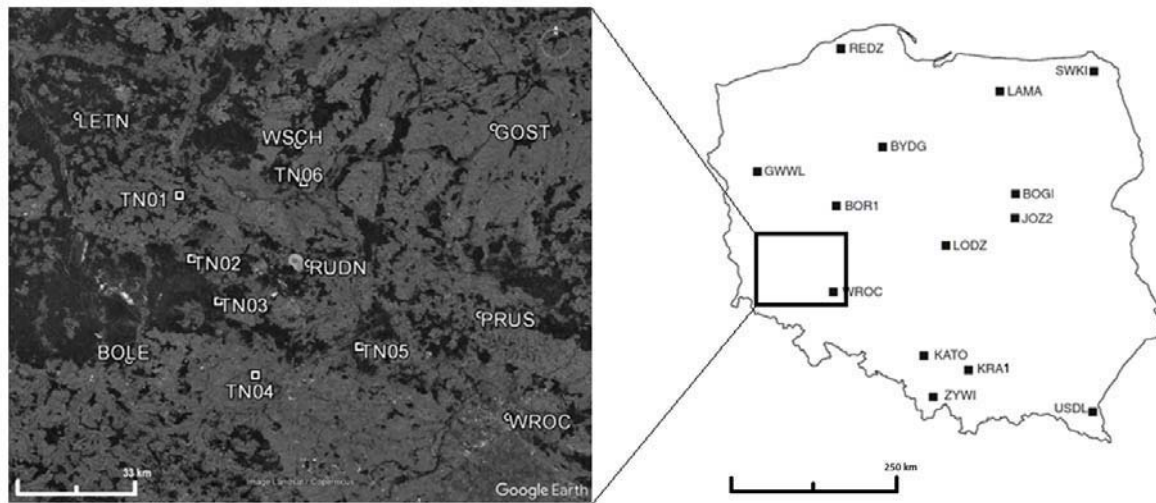
Fig. 1. Distribution of processed stations within Poland

The time span presented in this analysis includes one year (2015) of dual-frequency GPS observations. The satellite observation conditions can be considered to be optimal due to the utilization of observations from EPN. Post-processing using NAPEOS 3.3.1 was performed using a standard PPP strategy and a UD multi-station solution fixed to orbit/clocks, which enabled the GPS ambiguity fixing. As the true position, coordinates from the EPN cumulative solution C1934 were adopted and expressed at measurement epoch t_c and epoch 2011.0 consistent with the national PL-ETRF2000. In addition, the post-processing results were compared to the reference coordinates of the ASG-EUPOS network. The options selected for discussing the numerical tests are shown below:

- Final orbit and clock products from IGS and ESA; ESAs' IGS type products are processed by European Space Operations Centre (ESOC) using NAPEOS and were utilized in the study to check how product and model conformity affects the final accuracy,
- Antenna phase center offsets and variations corrected with IGS absolute phase center calibration file (igs08.atx),
- 10° cut-off elevation angle,
- 30 s data rate.

In the second numerical test, GNSS observations collected at 13 stations operating in south-west Poland were used (see Fig. 1 and Tab. 3). Seven stations belong to TPI NETpro network and ASG-EUPOS CORS network providing 24 hour per day observations and utilizing high class receivers with geodetic-grade choke ring antennas. Other stations were equipped with precise commercial surveying-grade receivers and antennas operating 8 hours per day. Among them, there are 3 stations (TN03, TN04 and TN05) for which only the relative calibrations model for GPS satellites were available for observations processing. The use of different classes antennas in the study is intended to determine the effect on positioning accuracy. In particular it is assumed that antennas with only relative PCO and PCV models will be characterized by lower accuracy of the final results.

Eight days of observations were registered between 15 and 22 July 2014 and were processed using PPP and UD multi-station pseudo-kinematic solutions dividing daily observations into various length: 2 hours, 1 hour and 30 minutes. The number of sessions analyzed in each strategy is presented in Table 4. All receivers provided dual-frequency (L1 and L2) GPS observations. Satellite observation conditions can be considered as optimal because the stations were located in open horizon area and the Position Dilution of Precision (PDOP) value did not exceed 2.5 during the entire measurement. Average PDOP for all stations is equal to 1.4 and none epochs were rejected due to high PDOP value during the processing. Reference (benchmark) ETRF2000 (epoch 2011.0) coordinates of seven TPI NETpro and ASG-EUPOS stations were adopted from their specifications (ASG-EUPOS; TPI NETpro). The "true" coordinates of stations TN01-TN06 were determined from an eight days cumulative network solution processed using NAPEOS.

Table 3. Observation sites' receivers and antennas

Network	Station	Receiver	Antenna and dome type	
TPI NETpro CORS	BOLE	Topcon NET-G3A	TPSCR.G5	TPSH
	GOST	Topcon NET-G3A	TPSCR.G5	TPSH
	LETN	Topcon NET-G3A	TPSCR.G5	TPSH
	PRUS	Topcon NET-G3A	TPSCR.G3	TPSH
	RUDN	Topcon NET-G3A	TPSCR.G5	TPSH
	WSCH	Topcon NET-G3A	TPSCR.G5	TPSH
ASG-EUPOS CORS	WROC	LEICA GR25	LEIAR25.R4	LEIT
Test network with commercial receivers	TN01	Trimble SPS 882	TRMR8_GNSS3	NONE
	TN02	Trimble SPS 882	TRMR8_GNSS3	NONE
	TN03	Topcon HIPER PRO	TPSHIPER_PLUS	NONE
	TN04	Topcon HIPER PRO	TPSHIPER_PLUS	NONE
	TN05	Topcon HIPER PRO	TPSHIPER_PLUS	NONE
	TN06	Trimble SPS 882	TRMR8_GNSS3	NONE

Table 4. Number of sessions per station analyzed in each processing strategy

	PPP solution			
	daily (24h)	**2 h**	**1 h**	**30 min**
CORS network	8	96	192	384
TN01-TN06 test network	8 (8 h)	32	64	128
	UD multi-station solution			
	daily (24 h)	**2 h**	**1 h**	**30 min**
CORS network	8	96	192	384
TN01-TN06 test network	8 (8 h)	32	64	128

4. NUMERICAL TESTS RESULTS

Starting with the first numerical test, Tables 5 and 6 present the statistics of differences between PPP solution results using IGS/ESA final products and reference coordinates from an EPN cumulative solution at the epoch of measurement: standard deviation (STD), mean coordinate differences and root mean square (RMS). Both solutions are characterized by a very high precision of horizontal coordinates depicted by STD, ranging from 1.1 mm to 2.7 mm for IGS and from 1.8 mm to 2.9 mm for ESA. According to common knowledge about PPP, the North component is determined slightly more precisely than the East component for IGS. However, this principle is not so obvious for solutions utilizing ESA products. Regarding the horizontal coordinates, differences in northing are characterized by offsets varying in the range of -3.6 mm to 0.4 mm (IGS) while for East, the mean differences range from -1.7 mm to 2.6 mm. Referring to ellipsoidal height (ΔU) determination statistics, the results are less satisfying than the horizontal results: the STD amounted to about 5-7 mm (with the exception of the KRA1 where two protruding epochs have doubled this indicator twice) and mean differences slightly exceeded $\pm$ 10 mm in some cases. In the KRA1 chart (Fig. 2), two significantly departing epochs are visible. The offset from a reference height exceeding 10 cm occurred on days 28 and 285 of the year 2015 (DOY). In post-processing covering these two days, about 10% of observations from KRA1 were rejected at the stage of least square estimation, while for other days this factor varies around 2%. The lack of clear conclusions from the pre-processing screening and the incomplete set of the observed satellites (relative to other days of processing) as well as the exclusion of these two epochs from the EPN cumulative solution suggest that problems arise during registration of observations at the station. After excluding these two epochs from analysis, the maximum height difference did not exceed $\pm$ 30 mm. The discrepancy between IGS and ESA PPP mean differences is insignificant: mean North differences from the IGS solution are about 1 mm closer to true position, while the mean ellipsoidal height differences are 1 mm better for ESA.

Table 5. The accuracy statistics for IGS PPP daily solution (epoch t_c) at the processed sites [mm]

IGS PPP

STATION	STD			Mean differences			RMS		
	ΔN	ΔE	ΔU	ΔN	ΔE	ΔU	ΔN	ΔE	ΔU
BOGI	1.2	1.9	5.5	-2.1	-0.9	-2.7	2.5	2.0	6.2
BOR1	1.2	1.9	5.3	-3.2	0.6	-3.9	3.4	2.0	6.6
BYDG	1.4	1.7	6.3	-1.2	-0.7	-6.3	1.8	1.9	8.9
GWWL	1.8	1.8	6.0	0.4	-1.4	-10.8	1.9	2.3	12.4
JOZ2	1.4	1.8	5.8	-2.5	0.3	-4.7	2.9	1.8	7.5
KATO	1.8	2.7	5.4	-2.1	0.7	-11.0	2.7	2.7	12.3
KRA1	1.9	2.4	12.3	-2.7	1.3	-6.1	3.3	2.7	13.8
LAMA	1.3	1.6	5.8	-1.7	0.5	-4.5	2.1	1.7	7.4
LODZ	1.4	1.7	6.0	-2.1	-1.9	-7.4	2.5	2.6	9.5
REDZ	1.4	1.6	6.5	-2.2	1.2	-7.2	2.6	2.0	9.7
SWKI	1.1	2.1	5.8	-2.3	2.6	-4.0	2.6	3.4	7.1
USDL	1.3	1.9	6.1	-3.6	-1.7	-8.3	3.8	2.5	10.4
WROC	1.2	1.9	5.2	-1.5	-0.3	-9.5	1.9	1.9	10.8
ZYWI	1.4	2.2	6.6	-2.6	-1.4	-8.1	2.9	2.6	10.5
MEAN	1.4	1.9	6.3	-2.1	-0.1	-6.7	2.6	2.3	9.5

Table 6. The accuracy statistics for ESA PPP daily solution (epoch t_c) at the processed sites [mm]

ESA PPP

STATION	STD			Mean differences			RMS		
	ΔN	ΔE	ΔU	ΔN	ΔE	ΔU	ΔN	ΔE	ΔU
BOGI	1.9	1.9	5.7	-3.0	-1.3	-1.6	3.5	2.3	5.9
BOR1	1.8	1.9	5.5	-4.1	0.1	-2.7	4.5	1.9	6.1
BYDG	2.0	2.0	6.4	-2.1	-1.1	-5.2	2.9	2.3	8.3
GWWL	2.2	1.9	6.2	-0.4	-1.9	-9.7	2.2	2.7	11.6
JOZ2	2.1	1.9	6.0	-3.5	-0.2	-3.5	4.1	1.9	7.0
KATO	2.7	2.9	5.5	-2.9	0.2	-9.8	3.7	2.9	11.3
KRA1	2.2	2.4	12.3	-3.7	0.7	-5.4	4.3	2.5	13.4
LAMA	1.9	1.9	5.8	-2.7	0.0	-3.5	3.3	1.9	6.8
LODZ	1.9	2.0	6.1	-3.0	-2.4	-6.3	3.6	3.1	8.8
REDZ	2.2	1.7	6.6	-3.2	0.9	-6.1	3.8	1.9	9.0
SWKI	1.8	2.3	5.9	-3.3	2.2	-3.0	3.7	3.2	6.7
USDL	2.0	2.1	6.3	-4.6	-2.2	-7.3	5.0	3.0	9.7
WROC	2.0	2.2	5.5	-2.3	-0.8	-8.4	3.0	2.3	10.0
ZYWI	2.1	2.4	6.8	-3.5	-1.9	-7.0	4.1	3.1	9.7
MEAN	2.0	2.1	6.5	-3.0	-0.5	-5.7	3.7	2.5	8.9

Figure 2 shows the epoch-wise differences between IGS PPP solution and true coordinates. The presented charts indicate the high repeatability of daily solutions, particularly for horizontal coordinates whose mean offsets did not exceed ± 10 mm during the whole year of processed observations. For the height component, it can be seen that fluctuations at all stations correspond to each other and may have a seasonal character, probably related to used tropospheric delay. The predominance of negative values among height mean differences may also come from the use of the tropospheric model (see Processing Strategy section). As the day-by-day solutions from other processing strategies (IGS FIX, ESA PPP, ESA FIX) are very similar to the one shown in Figure 2, their presentation was omitted to maintain the compactness and transparency of analysis.

Table 7 presents STDs and the mean position differences obtained in UD multi-station (FIX) solutions using IGS and ESA orbits and clocks. In comparing the results, one can conclude that only East precision is slightly superior to that obtained from PPP for both IGS and ESA solutions. This confirms the thesis that for daily observations the accuracy of both undifferentiated float (PPP) and fixed ambiguity solutions are equivalent. Fixing the ambiguities slightly affected the East mean values of the coordinate differences as well.

Table 7. The STD and mean differences for IGS FIX and ESA FIX daily solutions (epoch t_c) [mm]

|	IGS FIX						ESA FIX					
	STD			Mean differences			STD			Mean differences		
STATION	ΔN	ΔE	ΔU	ΔN	ΔE	ΔU	ΔN	ΔE	ΔU	ΔN	ΔE	ΔU
BOGI	1.1	1.3	5.6	-2.1	1.1	-1.2	1.9	1.6	5.8	-3.0	0.6	-0.1
BOR1	1.1	1.3	5.2	-3.3	0.2	-3.9	1.8	1.6	5.3	-4.2	-0.2	-2.8
BYDG	1.4	1.2	6.5	-1.1	-0.2	-6.8	1.9	1.5	6.5	-2.1	-0.6	-5.7
GWWL	1.9	1.5	6.0	-0.1	0.5	-10.9	2.2	1.7	6.2	-1.0	0.1	-9.8
JOZ2	1.3	1.6	5.9	-2.7	-0.2	-4.2	2.1	1.8	6.1	-3.6	-0.7	-3.1
KATO	1.8	1.5	5.3	-2.1	-0.4	-11.1	2.6	1.9	5.4	-3.0	-0.9	-10.0
KRA1	1.8	1.7	11.4	-2.9	-0.1	-8.1	2.2	1.8	11.6	-3.9	-0.6	-7.3
LAMA	1.2	1.4	5.9	-1.8	0.7	-3.4	1.9	1.6	5.8	-2.8	0.3	-2.4
LODZ	1.4	1.2	5.9	-2.3	-0.9	-5.7	1.9	1.6	6.2	-3.2	-1.4	-4.6
REDZ	1.3	1.3	6.1	-1.9	0.3	-7.4	2.1	1.4	6.1	-2.8	0.0	-6.3
SWKI	1.1	1.5	5.8	-2.1	0.8	-5.3	1.8	1.7	6.0	-3.2	0.4	-4.2
USDL	1.3	1.3	6.0	-3.6	-1.7	-8.3	1.9	1.6	6.2	-4.5	-2.2	-7.3
WROC	1.2	1.4	5.2	-1.1	0.4	-11.2	1.9	1.6	5.6	-2.0	-0.1	-10.0
ZYWI	1.3	1.6	6.5	-2.5	-1.6	-7.9	2.0	2.0	6.7	-3.4	-2.1	-6.7
MEAN	1.4	1.4	6.2	-2.1	-0.1	-6.8	2.0	1.7	6.4	-3.0	-0.5	-5.7
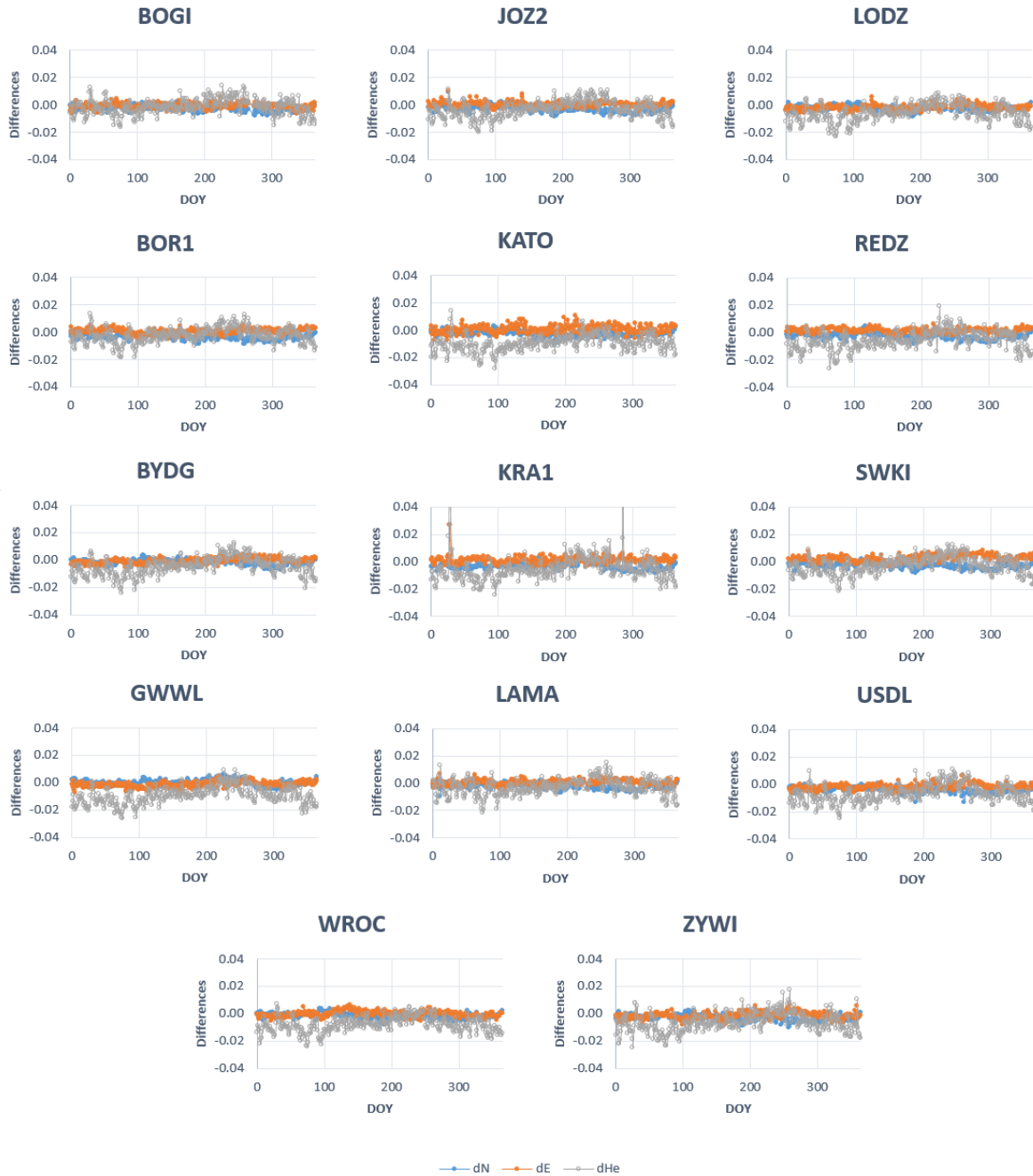
Fig. 2. North, East and ellipsoidal height epoch-wise differences [m] from IGS PPP processing at epoch t_c

In analyzing the UD positioning solutions capability to determine coordinates in national ETRF2000 realizations, it should be noted that despite small velocities in this frame, coordinates must be expressed at a specific epoch. In the study, using observations from EPN stations enables expressing a determined position to the desired epoch using station intraplate velocities. However, in the processing of observations from receivers operating at unknown positions, the velocity field, which is determined in cumulative solutions from several years of observations, is not known. Thus, in the analysis no compensation related to ETRF velocities was used for this set of stations. Table 8 presents the accuracy of statistics resulting from references obtained in processing positions to a cumulative EPN solution in ETRF2000 expressed at epoch 2011.0 and, therefore, compatible with Polish national reference frame regulations. The adjustment of reference coordinates to the 2011.0 epoch significantly

affected mean differences at stations characterized by the highest velocity and vertical movement values (see Table 2), like KATO, where North mean differences increased from -2.1 mm to -18.8 mm and SWKI where ellipsoidal height mean differences increased from -4.0 mm to -13.8 mm (Table 5 and 8). For other stations characterized by negligible velocities corrections are a few times smaller than GNSS positioning accuracy. However, for the height component characterized by greater dynamics, the deterioration of the results is noticeable. In statistics, where the resulting positions are referenced to ASG-EUPOS catalogue coordinates, the mean differences are even greater and equal more than 20 mm referring to ellipsoidal heights, what is probably due to the lower accuracy of reference coordinates. However, it should be noted that the change of coordinates in the studied data set refers to more than a four-year period between the measurement epoch and the reference epoch. A continuous change of coordinates over time, although small for Poland, will increase with the increase of the difference between the measurement epoch and the reference epoch.

Table 8. The accuracy statistics for the IGS PPP solution after expressing reference coordinates from EPN and ASG-EUPOS at epoch 2011.0 [mm]

	IGS PPP					
	Mean differences (EPN)			**Mean differences (ASG)**		
STATION	ΔN	ΔE	ΔU	ΔN	ΔE	ΔU
BOGI	-1.3	-2.1	-5.9	-4.0	-1.1	-8.5
BOR1	-3.6	-0.7	-8.6	-5.2	1.4	-16.3
BYDG	-2.5	-2.6	-9.1	-4.2	-1.3	2.7
GWWL	-1.9	-2.9	-17.9	-2.3	-0.1	9.0
JOZ2	-2.8	-0.3	-7.1	-4.3	0.7	-8.2
KATO	-18.8	1.3	-19.2	-19.3	1.9	-23.5
KRA1	-3.0	0.7	-8.5	-2.0	2.0	-12.7
LAMA	-1.4	-0.7	-8.4	-5.5	-0.3	-10.6
LODZ	-2.4	-1.2	-10.9	-1.6	0.9	0.3
REDZ	-3.6	0.2	-9.9	-2.4	0.4	1.6
SWKI	-2.6	-0.4	-13.8	-0.5	0.4	-10.4
USDL	-3.5	-2.4	-13.6	-3.5	-2.7	-0.5
WROC	-1.3	-2.8	-12.2	-1.2	-4.2	-20.9
ZYWI	-1.3	-2.3	-11.9	-3.8	-1.4	-5.0
MEAN	-3.6	-1.2	-11.2	-4.3	-0.3	-7.3

Position and height differences for sub-daily observing sessions from the network composed of geodetic and surveying-grade GNSS receivers/antennas are presented in Tables 9, 10 and 11, as well as Figures 3 and 4. The upper values in Tables rows describes the results from PPP, while the lower ones depict the UD network results. The degradation of positioning precision depicted by the STD occurs with the shortening of the observation session, particularly for the PPP solution. The horizontal PPP STDs below ± 10 mm for all stations occurred in sessions longer than 2 hours of observation. For shorter periods the precision decreases, although the North and East components do not exceed a 15 mm threshold for almost all analyzed stations. The exception is TN03 where STD increased to 22 mm. Concerning the height STD it can be seen that precision is 1.5-2 times lower, rising to nearly 30 mm (TN03) in the 30 minutes session. The difference in both horizontal and vertical STD

values between geodetic-grade and surveying-grade receivers/antennas is slight but noticeable, particularly in case of receivers with relative antenna calibration models (TN03 to TN05). Referring to the UD multi-station solution, it provides an improvement in North, East and in most cases height determination. The greatest advancement has been noted in easting component where for sub-daily sessions the STD improved from 32% to 70%. Fixing the ambiguity in UD multi-station solution contribute to precision below 10 mm for horizontal coordinates in almost all analyzed time series. The advantage of UD multi-station solution over PPP blurs with the extension of the observation time.

Table 9. RMS values from PPP / UD multi-station solutions for sub-daily observing sessions [mm]

IGS PPP/FIX RMS

station		24 h / 8 h			2 h			1 h			30 min		
		ΔN	ΔE	ΔU	ΔN	ΔE	ΔU	ΔN	ΔE	ΔU	ΔN	ΔE	ΔU
BOLE	PPP	1.7	5.0	26.4	5.2	6.0	26.5	6.7	7.6	31.3	10.2	8.8	32.2
	FIX	2.0	3.5	26.3	4.4	4.0	26.6	5.4	5.1	29.2	7.8	5.3	30.1
GOST	PPP	4.6	2.5	19.8	5.9	4.7	21.3	7.1	7.5	23.6	9.2	8.1	25.7
	FIX	4.4	1.5	19.6	5.8	2.5	20.6	6.4	3.3	22.3	7.7	3.9	22.9
LETN	PPP	1.7	1.6	24.8	4.4	5.0	27.3	9.0	9.4	31.8	9.5	10.8	32.9
	FIX	1.8	2.3	22.9	4.8	3.5	25.8	5.5	4.0	26.6	7.0	4.7	26.2
PRUS	PPP	5.0	5.0	20.2	6.8	7.4	20.9	7.5	8.8	29.0	10.8	10.6	29.0
	FIX	5.1	2.4	18.1	6.3	3.5	19.7	6.6	4.1	23.5	7.5	4.8	23.3
RUDN	PPP	3.7	5.4	22.5	5.9	6.8	24.8	7.6	8.3	26.1	9.1	11.2	28.2
	FIX	3.8	2.7	23.9	5.7	4.2	23.2	7.0	5.4	24.4	8.3	7.5	25.2
WSCH	PPP	8.2	3.0	26.1	10.0	5.6	26.6	9.4	7.3	30.3	10.8	8.6	29.5
	FIX	8.0	2.3	25.0	9.0	3.7	26.1	9.0	4.2	28.1	9.7	4.8	28.6
WROC	PPP	4.8	4.6	13.6	6.7	5.6	15.2	7.6	7.0	16.7	8.7	7.5	18.0
	FIX	4.6	5.0	14.2	5.3	4.8	14.7	6.2	6.0	14.8	6.9	6.2	16.2
TN01	PPP	5.0	6.2	11.9	6.3	8.1	14.5	11.2	9.2	13.2	13.6	11.6	19.3
	FIX	4.4	2.2	12.3	5.2	3.2	13.3	7.1	3.9	15.6	8.2	4.3	19.0
TN02	PPP	6.3	4.3	9.1	7.8	8.6	14.3	10.6	7.5	13.3	13.9	7.8	21.4
	FIX	4.3	1.4	15.1	5.4	3.3	15.3	6.3	4.1	18.3	7.3	4.9	20.3
TN03	PPP	11.7	10.2	17.3	10.4	13.8	24.1	13.0	14.9	21.7	18.2	26.6	28.7
	FIX	7.4	6.1	17.8	7.6	7.6	16.8	9.9	7.4	24.0	12.5	9.3	26.1
TN04	PPP	9.6	15.6	19.4	10.8	15.2	21.6	11.6	17.4	21.6	12.8	18.9	23.3
	FIX	9.6	9.7	20.5	10.1	9.1	20.7	10.4	9.8	22.0	10.8	10.0	23.1
TN05	PPP	12.1	12.6	11.8	12.1	13.2	11.1	15.4	14.7	14.4	16.9	15.1	17.3
	FIX	10.2	10.3	14.8	10.5	10.7	15.3	12.1	10.6	19.7	12.8	10.8	23.8
TN06	PPP	9.0	3.8	11.8	10.8	7.2	12.4	15.0	10.0	13.3	18.6	14.0	18.8
	FIX	8.4	3.7	11.4	9.4	5.0	11.3	10.4	5.3	16.0	11.4	5.8	18.0

Table 10. STD values from PPP / UD multi-station solutions for sub-daily observing sessions [mm]

IGS PPP/FIX STD

station		24 h / 8 h			2 h			1 h			30 min		
		ΔN	ΔE	ΔU	ΔN	ΔE	ΔU	ΔN	ΔE	ΔU	ΔN	ΔE	ΔU
BOLE	PPP	0.5	1.3	3.9	4.9	3.7	8.4	6.5	6.4	11.9	10.1	7.5	15.1
	FIX	0.8	1.2	3.3	4.0	2.3	6.7	5.0	3.9	10.7	7.6	4.0	12.5
GOST	PPP	1.2	2.5	3.2	4.4	4.7	10.5	6.1	7.3	15.2	8.3	8.1	16.8
	FIX	0.8	1.2	4.3	3.9	2.4	10.0	4.7	3.2	12.6	6.2	3.9	13.7
LETN	PPP	1.1	1.7	4.7	4.3	5.0	13.7	9.0	9.4	21.3	9.5	10.8	22.5
	FIX	1.0	1.1	4.1	4.5	2.8	12.0	5.2	3.4	14.9	6.8	4.3	17.0
PRUS	PPP	1.3	2.0	4.9	4.9	5.7	10.9	7.0	7.1	18.5	10.6	9.3	18.6
	FIX	1.2	1.1	4.2	3.8	2.7	8.6	4.8	3.4	14.6	6.1	4.2	14.3
RUDN	PPP	1.0	3.1	5.7	4.8	5.3	11.8	6.7	6.9	13.5	8.2	10.2	16.2
	FIX	0.7	1.6	3.9	4.4	3.4	8.7	5.8	4.7	11.0	7.1	6.9	12.6
WSCH	PPP	1.2	2.8	4.5	6.2	5.6	11.1	5.7	7.4	14.5	7.2	8.6	15.6
	FIX	0.8	1.1	4.4	4.0	3.1	7.6	4.4	3.7	10.9	5.4	4.4	12.8
WROC	PPP	1.2	2.8	3.9	4.8	4.9	10.2	5.8	6.3	10.8	7.1	6.8	14.9
	FIX	1.6	1.6	4.1	3.4	2.9	6.9	4.5	3.9	7.8	5.4	4.3	11.6
TN01	PPP	2.5	5.8	9.1	4.3	7.8	13.1	8.1	9.3	13.3	10.2	11.3	18.4
	FIX	2.2	2.0	6.4	4.2	3.0	11.3	5.8	3.9	12.8	7.1	4.3	16.8
TN02	PPP	2.5	3.9	8.8	5.2	8.5	14.5	8.6	7.6	13.5	11.0	7.7	20.3
	FIX	2.6	1.5	9.8	4.0	3.3	13.9	5.1	4.1	15.2	6.3	4.9	17.6
TN03	PPP	6.1	5.7	9.1	7.1	6.1	24.6	9.3	7.2	21.4	13.0	22.0	28.7
	FIX	2.1	1.7	8.2	4.5	2.9	10.6	7.5	3.8	20.1	10.7	6.7	20.8
TN04	PPP	2.7	5.5	6.0	4.8	6.1	10.6	7.9	7.4	13.6	10.3	8.7	17.3
	FIX	1.8	1.7	6.9	3.9	2.6	8.3	5.5	3.7	10.4	6.6	4.1	12.7
TN05	PPP	2.5	2.8	7.0	5.2	3.9	10.4	9.1	6.6	13.1	11.2	7.2	15.9
	FIX	1.6	1.4	5.4	4.2	2.5	9.7	6.5	3.2	12.8	8.3	4.2	17.5
TN06	PPP	1.0	3.4	10.8	4.7	7.2	12.6	10.4	9.2	12.7	14.0	12.6	15.9
	FIX	2.1	3.3	9.4	4.5	4.5	11.5	6.1	4.9	15.7	7.4	5.5	17.7

During the analysis of the mean differences (cf. Table 11), it can be seen that the results for individual stations time series are close to each other. In case of geodetic-grade receivers/antennas horizontal coordinates exceed ± 5 mm threshold only for WSCH. The predominance of negative values, particularly in North is noticeable and may be associated with both intraplate velocities and reference coordinates errors. Referring to height mean differences, they range from -17.7 mm to -26.2 mm for TPI NETpro stations while for WROC it is equal to about -13 mm and consistent with results from previous EPN processing. This suggests a lack of consistency in the height system associated with the reference coordinates of TPI NETpro stations. For surveying-grade receivers the stations TN03-TN05 are characterized by greatest shifts from reference coordinates, up to ± 17 mm in horizontal and ± 20 mm in vertical plane. These are stations utilized receivers with relative antenna calibration models.

Table 11. Mean differences values from PPP / UD multi-station solutions for sub-daily observing sessions [mm]

IGS PPP/FIX MEAN DIFFERENCES

station		24 h / 8 h			2 h			1 h			30 min		
		ΔN	ΔE	ΔU	ΔN	ΔE	ΔU	ΔN	ΔE	ΔU	ΔN	ΔE	ΔU
BOLE	PPP	-1.6	-4.8	-26.2	-1.8	-4.7	-25.2	-1.6	-4.1	-29.0	-1.2	-4.7	-28.5
	FIX	-1.8	-3.4	-26.1	-1.9	-3.3	-25.7	-2.1	-3.3	-27.2	-1.8	-3.5	-27.3
GOST	PPP	-4.5	-0.7	-19.5	-5.0	-0.5	-18.5	-3.8	-1.7	-18.1	-4.0	-0.9	-19.5
	FIX	-4.4	-1.0	-19.2	-4.4	-0.8	-18.0	-4.4	-0.9	-18.4	-4.6	-0.8	-18.4
LETN	PPP	-1.3	-0.1	-24.4	-1.3	-0.8	-23.7	-0.5	-0.7	-23.7	-1.0	-0.5	-24.0
	FIX	-1.6	-2.1	-22.6	-1.7	-2.1	-22.9	-1.5	-2.0	-22.0	-1.4	-1.8	-19.9
PRUS	PPP	-4.9	-4.6	-19.6	-4.7	-4.8	-17.9	-2.8	-5.3	-22.4	-1.9	-5.0	-22.2
	FIX	-5.0	-2.2	-17.7	-5.1	-2.2	-17.7	-4.5	-2.3	-18.5	-4.4	-2.3	-18.4
RUDN	PPP	-3.6	-4.6	-21.8	-3.4	-4.3	-21.8	-3.6	-4.6	-22.4	-4.0	-4.6	-23.1
	FIX	-3.8	-2.2	-23.6	-3.7	-2.5	-21.5	-3.9	-2.7	-21.8	-4.2	-2.9	-21.8
WSCH	PPP	-8.1	1.4	-25.7	-7.9	0.9	-24.2	-7.6	0.2	-26.6	-8.1	0.6	-25.1
	FIX	-8.0	-2.0	-24.6	-8.1	-2.1	-24.9	-7.9	-2.0	-25.9	-8.1	-2.1	-25.6
WROC	PPP	-4.7	-3.8	-13.1	-4.6	-2.9	-11.3	-4.8	-3.1	-12.8	-5.1	-3.1	-10.1
	FIX	-4.4	-4.8	-13.7	-4.1	-3.9	-13.0	-4.3	-4.5	-12.6	-4.3	-4.5	-11.3
TN01	PPP	-4.4	3.0	-8.3	-4.6	2.8	-6.7	-7.8	-0.6	1.4	-9.1	-2.8	6.1
	FIX	-3.9	1.0	-10.7	-3.2	1.2	-7.5	-4.2	0.7	-9.1	-4.2	0.7	-9.1
TN02	PPP	-5.8	2.3	-3.8	-5.8	2.1	2.0	-6.3	0.5	0.3	-8.6	-1.8	6.9
	FIX	-3.5	0.2	-11.9	-3.8	0.5	-7.1	-3.7	0.0	-10.4	-3.7	0.0	-10.1
TN03	PPP	-10.2	-8.7	-15.1	-7.8	-12.5	-0.4	-9.2	-13.0	-4.4	-12.7	-14.9	1.9
	FIX	-7.1	-5.9	-16.1	-6.2	-7.0	-13.2	-6.5	-6.3	-13.3	-6.6	-6.5	-15.8
TN04	PPP	-9.3	-14.7	-18.6	-9.7	-14.0	-18.9	-8.6	-15.8	-17.0	-7.8	-16.8	-15.7
	FIX	-9.4	-9.5	-19.5	-9.4	-8.8	-19.1	-8.8	-9.1	-19.5	-8.6	-9.1	-19.4
TN05	PPP	-11.8	-12.4	-9.9	-10.9	-12.6	-4.5	-12.4	-13.2	-6.3	-12.6	-13.3	-7.0
	FIX	-10.1	-10.2	-13.9	-9.7	-10.4	-12.1	-10.3	-10.1	-15.0	-9.8	-10.0	-16.3
TN06	PPP	-9.0	-2.1	-6.1	-9.8	-1.7	-1.0	-10.9	-4.1	4.1	-12.3	-6.4	10.1
	FIX	-8.1	2.1	-7.2	-8.3	2.4	-1.3	-8.5	2.1	-3.5	-8.7	2.2	-3.4

The horizontal differences in Fig. 3 clearly show the advantage of UD multi-station solution over the PPP. The vast majority of 2 hours PPP results are within ± 20 mm threshold. Only half an hour UD multi-station solutions are of similar quality. In contrast, for shortest PPP sessions outliers close to even 6 cm can be seen. Analyzing ellipsoidal height epoch-wise differences depicted in Figure 4, it can be concluded that only sessions longer than 2 hours provided adequate repeatability of results which are within ± 4 cm range.
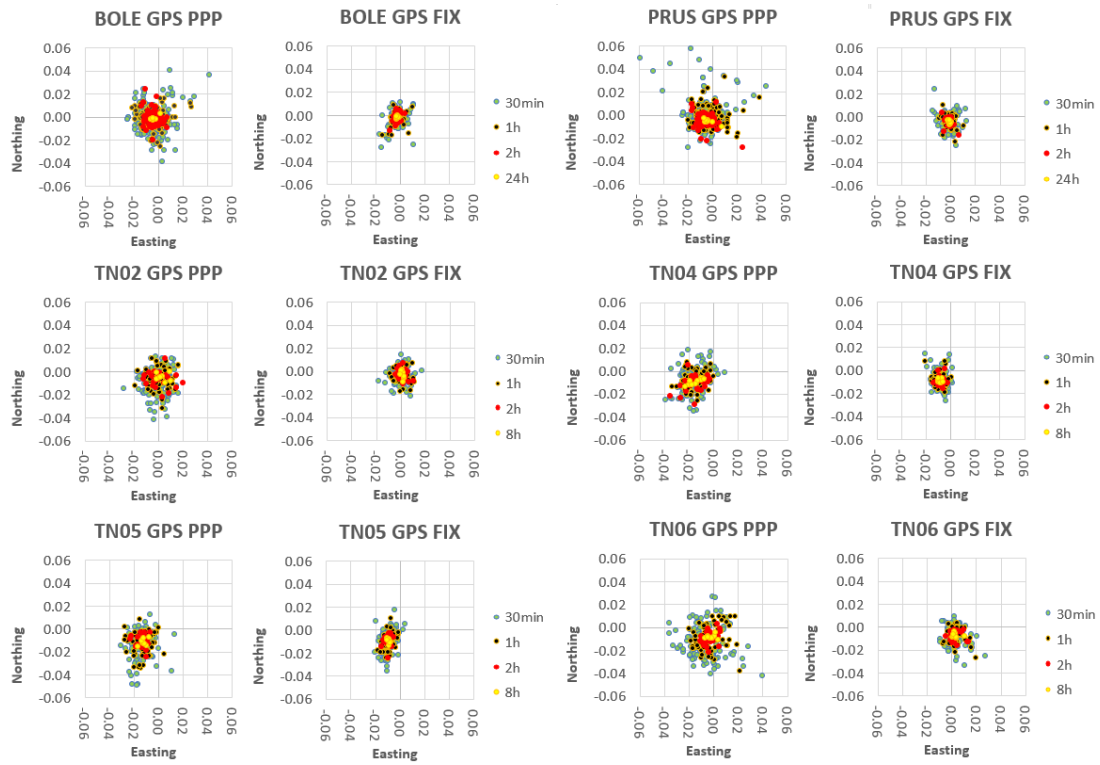
Fig. 3. Horizontal positioning differences [m] from IGS PPP and UD multi-station solutions for sub-daily observing sessions at chosen stations

Fig. 4. Ellipsoidal height epoch-wise differences [m] from IGS PPP and UD multi-station solutions for sub-daily observing sessions at chosen stations

5. SUMMARY

In the presented study, UD satellite positioning methods were utilized to determine high accuracy coordinates in the national reference frame. One year of GPS observations registered at 14 class A EPN stations were post-processed using NAPEOS 3.3.1 software package. The results of PPP and UD multi-station solution, fixed to satellite orbits and clocks products from IGS and ESA, were subsequently transformed from ITRF2008 to ETRF2000 in the measurement epoch. Considering the results obtained at epoch t_c with respect to the EPN

cumulative solution, the horizontal coordinate accuracy was characterized by RMS below 5 mm for all stations and solutions. In height determination, RMS is diversified depending on the individual station and varies by about 5-15 mm. In analyzing the day-by-day performance, the vast majority of horizontal mean differences did not exceed ± 10 mm during the whole processed year. Regarding to vertical component, some fluctuations from -3 cm to 2 cm can be seen, which may be due to seasonal atmospheric disturbances. This seems most likely because it applies to all stations in the corresponding periods. However to confirm it, longer time span (maybe several years) should be analyzed.

The difference between IGS and ESA products solution is negligible – the former showed approx. 1 mm better northing average RMS, while the latter is characterized by a similarly small improvements in height determination. The UD multi-station solution for daily observation processing also resulted in negligible improvement of the easting component. However, for short observing sessions, analyzed in the second numerical test comprising 13 stations equipped with different classes of GNSS receivers/antennas, the advantage of solution utilizing ambiguity fixing contributed to significant improvement in positioning precision, providing 1 cm STD after only 30 minutes of observation time. In the PPP case the results of sub-daily solutions are slightly worse, although it also provided accuracy below 5 cm in all analyzed time series, what fulfills the requirements of many surveying tasks. Ellipsoidal height determination in both solutions is characterized by 1.5-2 time worse results, but for observation sessions longer than 2 hours the accuracy below 4 cm is also achievable.

Returning to the analysis of daily observations in the first numerical test, utilization of observations from EPN allows referencing the true ETRF2000 coordinates at epoch 2011.0 (realization in accordance with the Polish national reference frame) using intraplate velocities of the processed stations. The results confirm the high level of stability of horizontal ETRF2000 coordinates for most Polish EPN stations, which RMS still did not exceed the 5 mm threshold in 24 h sessions. The exception occurred at KATO, with significant displacement in the north-south plane, equals to nearly 20 mm. Due to the vertical movements which occurred between the reference epoch (2011.0) and measurement epoch, the mean coordinate differences also raised, although they did not exceed 20 mm. Furthermore, this shift will increase along with an increase in the time span between the epoch of measurement and epoch of reference positions. This situation would not be the case for relative positioning because observation would be automatically tied to the CORS reference frame at the adopted epoch. However, it should be noted that the ETRF2000 local velocity field results in CORS network distortion and the positioning error is absorbed by outdated CORS positions. This entails the necessity of periodically updating the catalogue positions of reference stations regarding relative positioning. For countries where the velocity field has significant values (in the vicinity of the Mediterranean Sea or in the region of Fennoscandia) the differences in time would be even greater. Nevertheless, for Poland, the obtained results of the presented UD solutions will satisfy the requirements of many surveying and engineering applications where position has to be expressed in national reference frame with an accuracy of a few centimeters.

Acknowledgement

REFERENCES:

Afifi A., El-Rabbany A., (2015). Performance Analysis of Several GPS/Galileo Precise Point Positioning Models. *Sensors*; vol. 15(6), pp.14701-14726

Alkan R. M., İlçi V., Ozulu I. M., Saka M. H., (2015). A comparative study for accuracy assessment of PPP technique using GPS and GLONASS in urban areas, *Measurement*, vol. 69, pp. 1-8

Altamimi, Z., Rebischung P., Métivier L., Xavier C., (2016). ITRF2014: A new release of the International Terrestrial Reference Frame modeling nonlinear station motions. *Journal of Geophysical Research Solid Earth*, vol. 121, pp. 6109–6131

Araszkiewicz A., Bogusz J., Figurski M., Szafranek K., (2010). Application of short-time GNSS solutions to geodynamical studies. *Acta Geodynamica et Geomaterialia*, vol. 7(3), pp. 295–302

ASG-EUPOS. Active Polish Reference Network, http://www.asgeupos.pl [Accessed: 5 January 2017]

Bisnath, S., Gao, Y., (2009). Current state of precise point positioning and future prospects and limitations. *Sideris M.G. (eds) Observing our Changing Earth. International Association of Geodesy Symposia*, vol. 133 , pp. 615-623

Blewitt G., (1989). Carrier Phase Ambiguity Resolution for the Global Positioning System Applied to Geodetic Baselines up to 2000 km. *Journal of Geophysical Research*, vol. 94(B8), pp. 10187-10203

Boehm, J., Niell A., Tregoning P.,Schuh H., (2006). Global Mapping Function (GMF): A new empirical mapping function based on numerical weather model data, *Geophys. Res. Lett.*, vol. 33(7)

Boehm, J., Heinkelmann R.,Schuh H., (2007). Short Note: A global model of pressure and temperature for geodetic applications. *Journal of Geodesy*, vol. 81(10), pp. 679-683

Bogusz, J., Figurski, M., Kontny, B., Grzempowski P., (2012). Unmodelled Effects in the Horizontal Velocity Field Determination: ASG-EUPOS Case Study. *Artificial Satellites*, 47(2), pp. 67-79

Bosy J., (2013). Global, Regional and National Geodetic Reference Frames for Geodesy and Geodynamics. *Pure and Applied Geophysics*, vol. 171(6), pp 783–808

Boucher, C. Altamimi, Z. (2011). *Memo: Specifications for reference frame fixing in the analysis of a EUREF GPS campaign* (online at: http://etrs89.ensg.ign.fr/memo-V8.pdf).

Cai Ch., Gao Y., (2007). Precise Point Positioning Using Combined GPS and GLONASS Observations. *Journal of Global Positioning System*, vol. 6(1), pp. 13-22

Chen W., Hu C. W., Gao S., Chen Y.Q., Ding X.L., (2009). Error Correction Models and their Effects on GPS Precise Point Positioning. *Survey Review*, vol. 41(313), pp. 238-252

Choy S., Zhang S., Lahaye F., Héroux P., (2013). A Comparison between GPS-Only and Combined GPS +GLONASS Precise Point Positioning. *Journal of Spatial Science*, vol. 58, pp. 169-190

Collins, P., (2008). Isolating and estimating undifferenced GPS Integer ambiguities. *Proceedings of ION-GNSS-2008 International Technical Meeting of the Satellite Division* , San Diego, California, pp. 720-732

Dawidowicz K., Krzan G., (2014), Accuracy of single receiver static GNSS measurements under conditions of limited satellite availability. *Survey Review*, vol. 46(337), pp. 278-287

El-Mowafy A., (2009). Alternative Postprocessing Relative Positioning Approach Based on Precise Point Positioning. *Journal of Surveying Engineering*, Vol. 135(2), pp. 56-65

El-Rabbany, A. (2006). Introduction to GPS: The Global Positioning System. 2nd revised edition. Artech House Publishers, Boston , USA . ISBN 1-59693-016-0

EPN, Position Time Series. Multi-year EPN Solution. http://www.epncb.oma.be/_productsservices/timeseries/ [Accessed: 5 January 2017]

ESOC 2009: NAPEOS mathematical models and algorithms. Technical report, Darmstadt, Germany, Navigation Support Office, ESA/ESOC, 2009. DOPS-SYS-TN-0100-OPS-GN

Gendt, G., Dick G., Soehne W., (1999). GFZ Analysis Center of IGS- Annual Report, *1998 IGS Technical Reports*, IGS Central Bureau, Jet Propulsion Laboratory, Pasadena, CA, (eds K. Gowey, R. Neilan, A. Moore), November, pp. 79-87

Ge M., Gendt G., Rothacher M., Shi C., Liu J., (2008). Resolution of GPS carrier-phase ambiguities in precise point positioning (PPP) with daily observations. *Journal of Geodesy*, vol. 82(7), pp. 389-399

Geng J., Teferle F.N., Shi C., Meng X., Dodson A.H., Liu J., (2009). Ambiguity resolution in precise point positioning with hourly data. *GPS solutions*, vol. 13(4), pp. 263–270

Geng J., Meng X., Teferle F.N., Dodson A.H., (2010). Performance of precise point positioning with ambiguity resolution for 1- to 4-hour observation periods. *Survey Review*, vol. 42(316), pp.155-165

Golaszewski P., Wielgosz P., Stepniak K., (2017). Intercomparison and validation of GNSS-IWV derived with G-Nut and Bernese software. *Proceedings of 10th International Conference on Environmental Engineering (ICEE) Selected papers* , 27–28 April 2017, Vilnius, Lithuania

Hofmann-Wellenhof B., Lichtenegger H. Collins J., (2003). Global Positioning System: Theory and Practice. Springer-Verlag Wein New York

IGS (2015). IGS site guidelines. Technical report, Pasadena, California, IGS Central Bureau, Jet Propulsion Laboratory, [Online] Available at: http://kb.igs.org/hc/en-us/articles/202011433-Current-IGS-Site-Guidelines. [Accessed 14 February 2017]

Kalita J., Rzepecka Z., Szuman-Kalita I., (2014). The application of Precise Point Positioning in Geosciences. *Proceedings of 9th International Conference on Environmental Engineering (ICEE) Selected papers,* 22–23 May 2014, Vilnius, Lithuania

Kleusberg, A., (1986). Ionospheric propagation effects in geodetic relative GPS positioning. *Manuscripta Geodaetica*, vol. 11, pp. 256-261

Kouba J., Heroux P., (2001). Precise Point Positioning Using IGS Orbit and Clock Products. *GPS Solutions*, Vol. 5(2), pp. 12-28

Laurichesse, D., Mercier F.. (2007). Integer ambiguity resolution on undifferenced GPS phase measurements and its application to PPP. *Proceedings of ION-GNSS-2007 20th International Technical Meeting of the Satellite Division*, Fort Worth, Texas, pp 839–848

Lichten, S. M., Bar-Sever Y. E., Bertiger E. I., Heflin M., Hurst K., Muellerschoen R., Wu S. C., Yunck T. P., Zumberge J. F., (1995). GIPSY-OASIS II: A High precision GPS Data processing System and general orbit analysis tool, Technology 2006, NASA Technology Transfer Conference, Chicago, Il., Oct. 24-26

Marty, J. C. (ed) (2009). Documentation algorithmique du programme GINS, Version 5 juillet 2009 (in French). http://www.igsac-cnes.cls.fr/documents/gins/GINS_Doc_Algo.html.

Neilan, R.E., Zumberge J. F., Beutler G., Kouba J., (1997). The International GPS Service: A global resource for GPS applications and research. *Proceedings of ION-GPS-97 10th International Technical Meeting of the Satellite Division of the Institute of Navigation*, Kansas City, Missouri, pp. 883-889

Petit G., Luzum B., (2010). IERS Conventions (2010). *IERS Technical Note 36. Verlag des Bundesamts fnr Kartographie und Geodssie*, Frankfurt am Main

Paziewski J., Sieradzki R., Baryla R., (2017). High-rate GNSS positioning for precise detection of dynamic displacements and deformations: methodology and case study results. *Proceedings of 10th International Conference on Environmental Engineering (ICEE) Selected papers*, 27–28 April 2017, Vilnius, Lithuania

Rabbou M. A., El-Rabbany A., (2015). PPP Accuracy Enhancement Using GPS/GLONASS Observations in Kinematic Mode. *Positioning*, vol. 6(1), pp. 1-6

Roberts G. W., Tang X., Brown Ch., (2015). A review of satellite positioning systems for civil engineering. *Proceedings of the Institution of Civil Engineers - Civil Engineering*, vol. 168(4), pp. 185-192

Schenewerk, M., Dillinger W., Mader G., (1999). NOAA/NGS Analysis Strategy Summary, *1998 IGS Technical Reports*, IGS Central Bureau, at JPL, (eds K. Gowey, R. Neilan, A. Moore), November, pp. 99- 105

Springer T., Dilssner F., Escobar D., Flohrer C., Otten M., Svehla D., Zandbergen R., (2011). NAPEOS: The ESA/ESOC tool for Space Geodesy Geophysical Research Abstracts, vol. 13, EGU2011-8287

TPI NETpro. Polish Nationwide network of GPS / GLONASS reference stations, https://global.topnetlive.com/poland [Accessed: Accessed 5 January 2017]

Szafranek, K., (2012). The problem of temporal validity of reference coordinates in the context of reliability of the ETRS89 system realization in Poland. *Artificial Satellites*, vol. 47(4), pp. 177-188

Zumberge, J. F., Heflin, M. B., Jefferson, D. C., Watkins, M. M., Webb, F. H., (1997). Precise point positioning for the efficient and robust analysis of GPS data from large networks. *Journal of Geophysical Research: Solid Earth*, vol. 102(B3), pp. 5005-5017